nature structural & molecular biology

Telomere protection by mammalian Pot1 requires interaction with Tpp1

Dirk Hockemeyer[1], Wilhelm Palm[1], Tobias Else[2], Jan-Peter Daniels[1,5], Kaori K Takai[1], Jeffrey Z-S Ye[3,5], Catherine E Keegan[4], Titia de Lange[1] & Gary D Hammer[2]

The shelterin complex at mammalian telomeres contains the single-stranded DNA–binding protein Pot1, which regulates telomere length and protects chromosome ends. Pot1 binds Tpp1, the shelterin component that connects Pot1 to the duplex telomeric DNA–binding proteins Trf1 and Trf2. Control of telomere length requires that Pot1 binds Tpp1 as well as the single-stranded telomeric DNA, but it is not known whether the protective function of Pot1 depends on Tpp1. Alternatively, Pot1 might function similarly to the Pot1-like proteins of budding and fission yeast, which have no known Tpp1-like connection to the duplex telomeric DNA. Using mutant mouse cells with diminished Tpp1 levels, RNA interference directed to mouse Tpp1 and Pot1, and complementation of mouse *Pot1* knockout cells with human and mouse Pot1 variants, we show here that Tpp1 is required for the protective function of mammalian Pot1 proteins.

Mammalian cells distinguish their natural chromosome ends from damaged DNA by the presence of specific proteins found only at telomeres[1]. One of the proteins implicated in telomere protection is the single-stranded telomeric DNA–binding protein Pot1[2–8]. The human and fission yeast Pot1 proteins were identified based on their sequence similarity to an OB fold in TEBPα[2]. Recently, crystallography has shown that the telomeric protein Tpp1 carries an OB fold with structural similarity to TEBPβ, and biochemical evidence has indicated that, like TEBPα and TEBPβ, Pot1 and Tpp1 bind DNA cooperatively *in vitro*[9]. Pot1 and Tpp1 are found within a larger telomere-specific complex, called shelterin[1]. Shelterin also contains Trf1 and Trf2, which anchor this complex to the double-stranded TTAGGG repeat array of mammalian chromosome ends. Tpp1 and Pot1 are linked to the duplex telomeric DNA–binding proteins through Tin2, a protein that bridges Trf1 and Trf2 and interacts with Tpp1 (refs. 10–15). Owing to these interactions, Pot1 not only interacts with single-stranded telomeric DNA but also accumulates along the duplex telomeric repeat array[16].

Gene deletion and RNA interference (RNAi) experiments have shown that the mammalian and fission yeast Pot1 proteins are important for telomere protection[2–8]. Upon deletion of the two Pot1 proteins of mice (Pot1a and Pot1b[6]), DNA damage factors assemble at chromosome ends, indicating that cells no longer distinguish telomeres from sites of DNA damage. Compromised function of Pot1a and Pot1b also impairs proliferation, induces endoreduplication and incites unscheduled DNA repair reactions at chromosome ends. Pot1a and Pot1b have distinct functions[6]. Pot1a, but not Pot1b, is required to mask telomeres from the DNA damage signaling pathways. Conversely, Pot1b, but not Pot1a, limits the formation of single-stranded DNA at the 3′ telomere terminus.

The interaction of human POT1 with TPP1 has previously been implicated in the regulation of telomere length[12,13,15,17], but the contribution of TPP1 to the protective activity of POT1 has remained unclear. Of note, a mouse strain with a mutation in the *Tpp1* gene, the acd (adrenocortical dysplasia) mouse[18], has a phenotype that is markedly different from those associated with deletion of the mouse Pot1 genes. Although the acd mutation leads to developmental defects and acd mice with certain genetic backgrounds die post-partum[18], the mutation does not elicit the early embryonic lethality or the telomere-deprotection phenotypes of the *Pot1a Pot1b* double-knockout strain[6]. These findings, and the apparent lack of a Tpp1-like interacting partner for fission yeast Pot1, contradict the idea that Pot1-mediated telomere protection requires Tpp1. Furthermore, telomere protection in budding yeast requires the Pot1-like Cdc13 protein, which, although part of a larger complex, is not connected to factors associated with the duplex telomeric DNA. Here we set out to determine whether Pot1 proteins protect telomeres in conjunction with Tpp1.

RESULTS

Tpp1's role in telomere binding of Pot1a and Pot1b

To examine the effect of the acd *Tpp1* mutation on telomere structure and function, *Tpp1*$^{acd/acd}$ mouse embryo fibroblasts (MEFs) were

[1]Laboratory for Cell Biology and Genetics, The Rockefeller University, 1230 York Avenue, New York, New York 10065, USA. [2]Department of Internal Medicine, Division of Metabolism, Endocrinology and Diabetes, University of Michigan Health System, 109 Zina Pitcher Pl., Ann Arbor, Michigan 48109-0789, USA. [3]Division of Hematology, New York University School of Medicine, 650 First Avenue, New York, New York 10016, USA. [4]Department of Pediatrics, Division of Genetics, University of Michigan, 1150 W. Medical Center Dr., Ann Arbor, Michigan 48109-0652, USA. [5]Current addresses: Sir William Dunn School of Pathology, University of Oxford, South Parks Road, OX1 3RE Oxford, UK (J.-P.D.) and Department of Oncology, Kaiser Permanente Medical Group, Santa Rosa, California 95403, USA (J.Z.-S.Y.). Correspondence should be addressed to T.d.L. (delange@mail.rockefeller.edu).

Received 3 January; accepted 8 June; published online 15 July 2007; doi:10.1038/nsmb1270

isolated from embryonic-day-13.5 embryos generated by *Tpp1*$^{acd/+}$ intercrosses, and the cells were immortalized with SV40 large T antigen (SV40-LT). The acd phenotype is caused by aberrant splicing of the *Tpp1* gene owing to a G→A transition 5 nucleotides (nt) beyond the splice donor site of exon 3 (ref. 18). This mutation results in the use of a cryptic splice donor site and is predicted to generate a truncated Tpp1 protein lacking part of the OB fold, the Pot1-binding domain and the Tin2-binding domain. Chromatin immunoprecipitation (ChIP) results indicated that, as expected, the ability of antibodies raised against human TPP1 to precipitate telomeric DNA was diminished by over ten-fold in newly established *Tpp1*$^{acd/acd}$ MEFs, whereas ChIPs for Trf1, Trf2 and Rap1 showed minor changes (**Fig. 1a**,**b**). The *Tpp1*$^{acd/acd}$ genotype affected both Pot1a and Pot1b, which showed approximately four-fold reduction in telomeric ChIP. Furthermore, the expression of Pot1a and Pot1b proteins was slightly lowered in *Tpp1*$^{acd/acd}$ cells (**Fig. 1c**). Although the decrease in the telomeric association of Pot1a and Pot1b is consistent with their recruitment through Tpp1, the data also suggest that *Tpp1*$^{acd/acd}$ cells have a considerable amount of residual Pot1a and Pot1b at their telomeres. We noted that *Tpp1*$^{acd/acd}$ cells cultured for prolonged periods (>30 population doublings (PD)) had amounts of Pot1a and Pot1b at the telomeres close to those of wild-type cells (**Fig. 1d**,**e**). Such improved Pot1 recruitment is likely to be due to the selective growth advantage afforded by fully protected telomeres (see below).

The residual Pot1a and Pot1b at the telomeres of *Tpp1*$^{acd/acd}$ cells could be explained if the acd mutation creates a hypomorphic allele of *Tpp1* rather than a null allele. We tested this possibility with three small hairpin RNAs (shRNAs). *Tpp1* shRNA 3 was inferred to have the strongest effect, on the basis of its reduction of the telomeric ChIP signal in wild-type MEFs (**Fig. 1d**,**e** and data not shown). *Tpp1* knockdown in *Tpp1*$^{acd/acd}$ cells that were grown for >30 PD lowered the telomeric binding of Pot1a and Pot1b, indicating that most of the residual Pot1a and Pot1b at telomeres of *Tpp1*$^{acd/acd}$ cells was recruited by Tpp1. These data are consistent with recently reported interactions of Pot1 proteins with Tpp1 (refs. 7,8). In addition to its effect on Pot1a and Pot1b, *Tpp1* knockdown reduced the association of Tin2

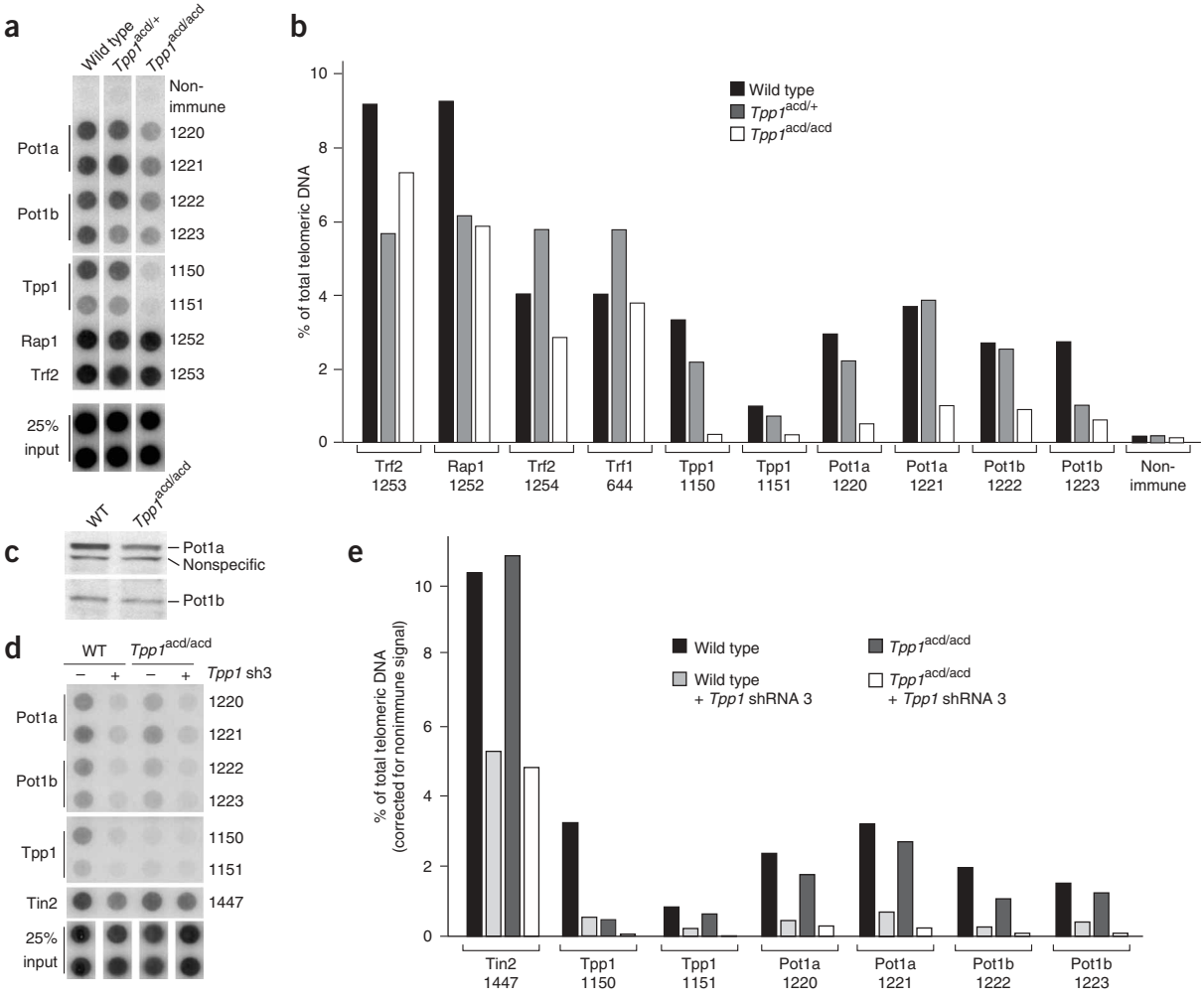

Figure 1 Dependence of Pot1a and Pot1b telomeric localization on Tpp1. (**a**) Telomeric DNA ChIP analysis of MEFs that are wild type, heterozygous or homozygous for the *Tpp1* acd allele. Cells had been cultured for ≤10 PD. Proteins and antibodies used in the ChIPs are indicated. None of the antibodies brought down nonspecific BamH1 repeat sequences used as a control (data not shown). (**b**) Quantification of data shown in **a**. (**c**) Immunoblots with antibodies 1221 and 1223 to detect Pot1a and Pot1b, respectively, in wild-type and *Tpp1*$^{acd/acd}$ cells. The nonspecific band serves as a loading control. (**d**) Telomeric DNA ChIP analysis of wild-type or *Tpp1*$^{acd/acd}$ MEFs transduced with *Tpp1* shRNA 3 (+) or a vector control (–) using antibodies against the indicated telomeric proteins. The numbers next to the radiograph specify the antibodies used. ChIPs were performed after 5 d of puromycin selection. The *Tpp1*$^{acd/acd}$ cells had been cultured for >30 PD. (**e**) Quantification of data shown in **d**.

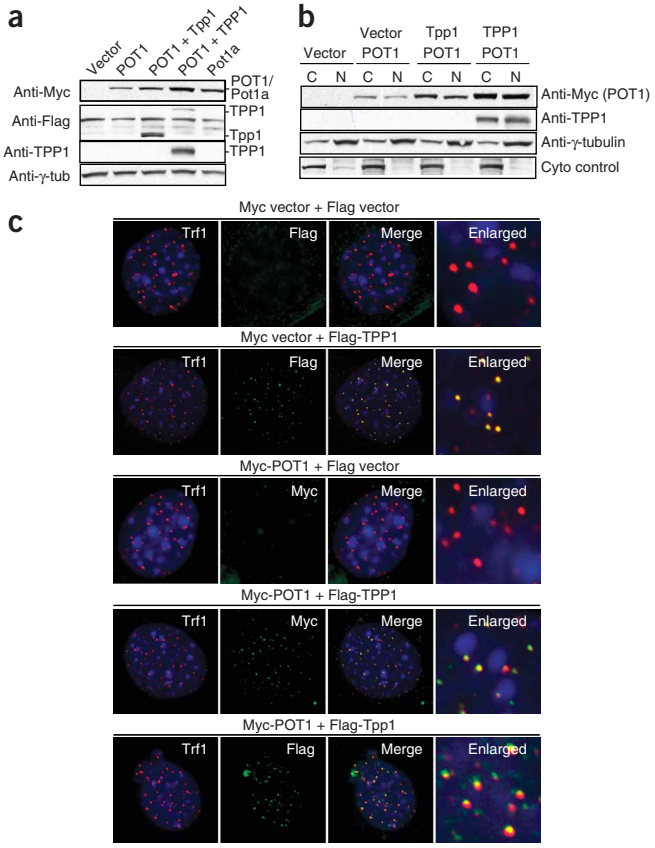

Figure 2 Human POT1 can be targeted to mouse telomeres by human TPP1. (**a**) Immunoblots of MEFs transduced with pWzl-N-MycPOT1 (human), pWzl-N-MycPot1a (mouse) or a vector control (pWzl-N-Myc) and subsequently transduced with pLPC-N-FlagTPP1 (human) or pLPC-N-FlagTpp1 (mouse), to express the proteins indicated above the lanes. We selected for pWzl and pLPC with hygromycin and puromycin, respectively. Proteins were detected with the indicated antibodies, with the following clone numbers: Myc, 9E10; human TPP1, 1151; Flag, M2; γ-tubulin, GUT88 (Sigma). (**b**) Subcellular fractionation of MEFs analyzed in the first four lanes in **a**. Human POT1 and TPP1 were detected using antibodies as in **a**, in cytoplasmic (C) and nuclear (N) fractions. The cytoplasmic control is a 30-kDa protein that cross-reacts with anti-Flag M2. (**c**) Immunofluorescence in MEFs transduced with retroviruses to express the indicated proteins, as in **a**. Antibodies were as follows: Trf1, 644 (red); Myc, 9E10 (green); Flag (M2; green). DNA was counter-stained with DAPI (blue).

with telomeres by about two-fold (**Fig. 1e**). This finding is consistent with previous data indicating that TPP1 has a stabilizing effect on TIN2 (ref. 19). Collectively, the Tpp1 shRNA data support the idea that acd is a hypomorphic allele of *Tpp1*. RT-PCR analysis showed a low amount of wild-type *Tpp1* messenger RNA in *Tpp1*$^{acd/acd}$ cells, despite the splice-site mutation (data not shown). Most probably, the hypomorphic nature of the acd mutation is due to expression of small amounts of Tpp1 from this mRNA.

Tpp1 binding–deficient Pot1 not detected at telomeres

The data above demonstrate that Tpp1 promotes the telomeric association of the mouse Pot1 proteins. These findings are consistent with a previous report that a POT1 variant with a point mutation in the TPP1-binding domain does not accumulate at telomeres[13]. However, it was recently reported that a form of mouse Pot1b lacking the C-terminal 300 amino acid residues can localize to telomeres despite its inability to bind Tpp1 (ref. 8). In contrast, our variants of Pot1b lacking either the C-terminal half (Pot1b-V2) or just the last 17 residues (Pot1b-623) were undetectable at telomeres, whereas full-length Pot1b showed the expected telomeric accumulation (**Supplementary Fig. 1a,b** online). However, the expression of these forms of Pot1b was low, and the proteins were largely excluded from the nucleus (**Supplementary Fig. 1c**), making the absence of telomeric staining difficult to interpret.

To further test whether Pot1 proteins might be able to bind telomeres in a Tpp1-independent manner, we turned to human POT1. When expressed in mouse cells, human POT1 did not accumulate at telomeres (**Fig. 2**). The lack of detectable telomeric binding was notable, as the expression level of POT1 was comparable to that of mouse Pot1a (**Fig. 2a**), which was readily detectable at telomeres (data not shown), and at least 50% of the POT1 protein appeared to reside in the nucleus, as indicated by subcellular fractionation (**Fig. 2b**). Coexpression of human POT1 with human TPP1 resulted in robust telomeric association of both proteins and also seemed to stabilize POT1 (**Fig. 2a,c**). Mouse Tpp1 could also promote the localization of human POT1 but seemed less active in this regard. Although Tpp1 was expressed in higher amounts than TPP1 (**Fig. 2a**), the signal of POT1 at telomeres appeared less prominent (**Fig. 2c** and data not shown) and the steady-state abundance of POT1 protein was lower (**Fig. 2a**). Coimmunoprecipitation experiments with human and mouse Pot1 and Tpp1 proteins from transiently transfected 293T cells also suggested that the interaction of mouse Tpp1 with human POT1 is weaker than the cognate interaction (**Supplementary Fig. 2** online). These data support the idea that Pot1 can be detected at telomeres by immunofluorescence only if it is able to interact with Tpp1. Accordingly, we found that the V2 truncation variant of human POT1, which lacks the C-terminal region and therefore does not bind TPP1, is not detectable at telomeres (**Supplementary Fig. 3** online). Subcellular fractionation indicated that this form of POT1 is largely excluded from the nucleus (**Supplementary Fig. 3**), but even when we forced its nuclear localization by adding a nuclear localization signal, it did not accumulate at telomeres (**Supplementary Fig. 3**). Collectively, these data underscore the conclusion that Tpp1 has a major role in the recruitment of Pot1 to telomeres and suggest that the single-stranded DNA–binding activity of Pot1 in itself is not sufficient to support normal Pot1 accumulation at chromosome ends. Although the results do not exclude the possibility that a minor fraction of Pot1 binds telomeres in a Tpp1-independent manner, the data below suggest that this binding mode (if it exists) is not sufficient for telomere protection.

Occasional telomere deprotection in *Tpp1*$^{acd/acd}$ cells

The telomeres of newly derived (<10 PD) *Tpp1*$^{acd/acd}$ cells had normal lengths, and there was no change in the relative abundance of the single-stranded telomeric DNA (see **Figs. 3** and **4**). The normal structure of the telomeres in *Tpp1*$^{acd/acd}$ cells contrasts with the two- to three-fold excess of single-stranded TTAGGG repeat DNA observed in *Pot1b* knockout cells[6]. However, *Tpp1*$^{acd/acd}$ cells did show a mild telomere-deprotection phenotype, as indicated by the occasional occurrence of telomere dysfunction–induced foci (TIFs). TIFs were detected using indirect immunofluorescence detection of γ-H2AX or 53BP1, in combination with markers of telomeric proteins or fluorescent *in situ* hybridization (FISH) of telomeric DNA. As expected, wild-type cells and cells heterozygous for the acd mutation did not contain an appreciable number of TIFs (<1% of cells had ten or more

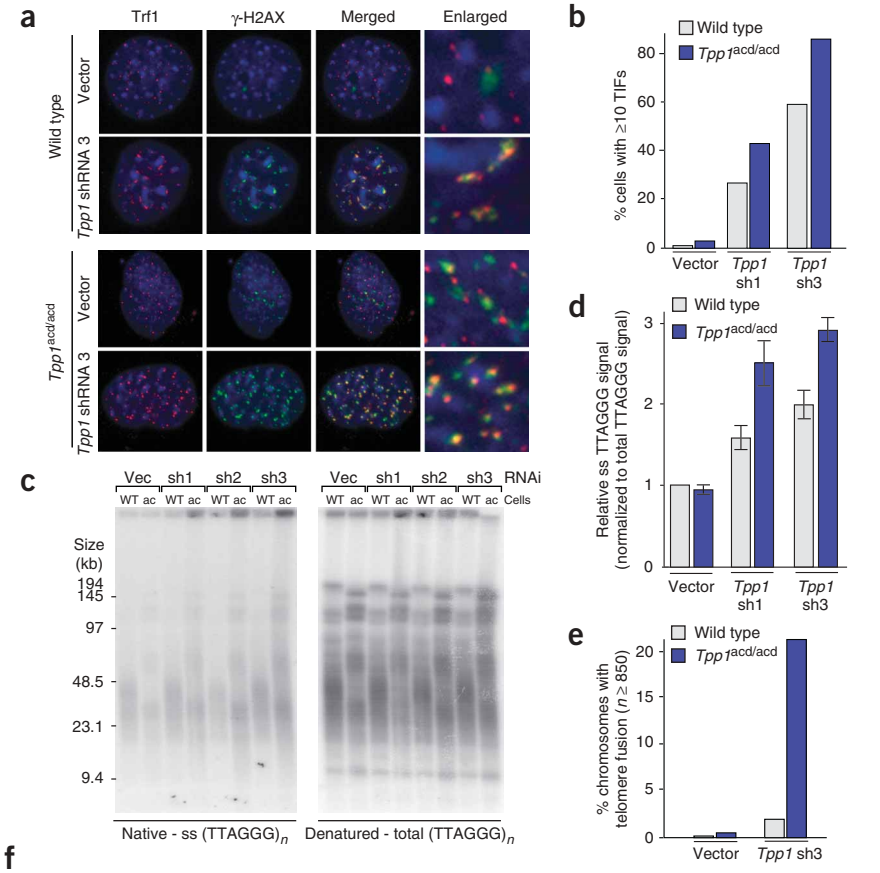

Figure 3 Telomere deprotection associated with reduced Tpp1 abundance. (**a**) Occurrence of TIFs upon *Tpp1* knockdown. MEFs of the *Tpp1* genotypes indicated at left were infected with *Tpp1* shRNA 3 or with control vector (pSuperior), selected for 4 d with puromycin, stained using immunofluorescence to detect TRF1 (antibody 644, red) and γ-H2AX (green), and counter-stained with DAPI (blue). Trf1 immunofluorescence signals are reduced in $Tpp1^{acd/acd}$ MEFs infected with *Tpp1* shRNAs. (**b**) Quantification of TIF-positive cells in **a**. Cells with ten or more Trf1 signals colocalizing with γ-H2AX foci were scored as TIF-positive. $n \geq 120$ cells for each experiment. (**c**) In-gel overhang assay of MEFs of wild-type (WT) and $Tpp1^{acd/acd}$ (ac) infected with *Tpp1* shRNA (sh) 1, 2 or 3, or with control vector. Left, detection of single-stranded (ss) $(TTAGGG)_n$ repeats; right, detection of both ss and double-stranded telomeric repeat segments after denaturation of the gel. (**d**) Quantification of mean overhang signals from three different wild-type or $Tpp1^{acd/acd}$ cell lines infected with the indicated shRNAs. Error bars represent s.d. (**e**) Quantification of telomere fusion frequency in MEFs of the indicated *Tpp1* genotypes infected with the indicated shRNAs or control vector. (**f**) Telomeric FISH analysis of metaphase chromosomes derived from cells of the indicated *Tpp1* genotypes infected with *Tpp1* sh3 or with control vector. Telomeric hybridization signal is shown in green and DAPI-stained chromosomes are colored in red.

TIFs; **Fig. 3a**,**b** and data not shown). However, a small fraction (2%–3%) of $Tpp1^{acd/acd}$ MEFs contained ten or more TIFs (**Fig. 3a**,**b**). This frequency of TIF-positive cells is low compared with the phenotype of *Pot1a* knockout cells or *Pot1a Pot1b* double-knockout cells (>70% of cells had ten or more TIFs[6]). Similarly, $Tpp1^{acd/acd}$ cells showed an increase in the frequency of telomere fusions (~10 fusions per 1,000 chromosomes in acd cells, compared with ~1 fusion per 1,000 chromosomes in wild-type cells), but this phenotype was less pronounced than of *Pot1a Pot1b* double-knockout cells (35 fusions per 1,000 chromosomes[6]). Furthermore, the acd mutation was associated with the occasional occurrence of tetraploid metaphases with diplochromosomes, a phenotype that is prominent in *Pot1a* knockout cells and *Pot1a Pot1b* double-knockout cells[6]. Tetraploid metaphase spreads composed of diplochromosomes occurred in ~5% of the $Tpp1^{acd/acd}$ cells (data not shown). Thus, $Tpp1^{acd/acd}$ MEFs have infrequent telomere-deprotection phenotypes, consistent with the diminished presence of Pot1a and Pot1b at their telomeres. Despite being mild, the telomere phenotype of $Tpp1^{acd/acd}$ cells might select for cells with enhanced Pot1 recruitment, explaining the presence of Pot1a and Pot1b at telomeres of $Tpp1^{acd/acd}$ cells cultured for >30 PD in amounts nearly the same as those seen in wild-type cells (see **Fig. 1**).

Tpp1 knockdown results resemble *Pot1a Pot1b* knockout

Knockdown of Tpp1 by RNAi in young $Tpp1^{acd/acd}$ cells or wild-type MEFs resulted in a phenotype similar to that of *Pot1a Pot1b* double-knockout cells. There was a strong induction of TIFs (**Fig. 3a**,**b**), the amount of single-stranded telomeric DNA was increased two- to three-fold (**Fig. 3c**,**d**), and there was a higher frequency of telomere fusions (~20% of chromosomes showing a telomere fusion; **Fig. 3e**,**f**). All three phenotypic characteristics were most prominent in $Tpp1^{acd/acd}$ cells treated with *Tpp1* shRNAs but also occurred when *Tpp1* was knocked down in wild-type cells.

The frequency of telomere fusions in $Tpp1^{acd/acd}$ cells treated with *Tpp1* shRNA 3 is three- to four-fold higher than in *Pot1a Pot1b* double-knockout cells. This result raised the concern that our *Pot1* knockout strategy might have generated hypomorphic rather than null alleles. To test this possibility, we targeted our Pot1 knockout cells with shRNAs specific to both *Pot1* genes and monitored the TIF response, which is a sensitive and quantitative assay (**Supplementary Fig. 4** online). Treatment with *Pot1a* shRNA did not increase the TIF response of *Pot1a* knockout cells, despite this shRNA's effectiveness in inducing TIFs in *Pot1b* knockout cells. Similarly, shRNA specific to *Pot1b* did not induce TIFs in *Pot1b* knockout cells, whereas it slightly increased the TIF response in *Pot1a* knockout cells. On the basis of this data, we consider it unlikely that our knockout strategy generated hypomorphic alleles of *Pot1a* and *Pot1b*. The alternative explanation for the increase in telomere fusions upon *Tpp1* knockdown is that loss of Tpp1 affects other components of the shelterin complex. Related to this, TPP1 has recently been shown to affect the

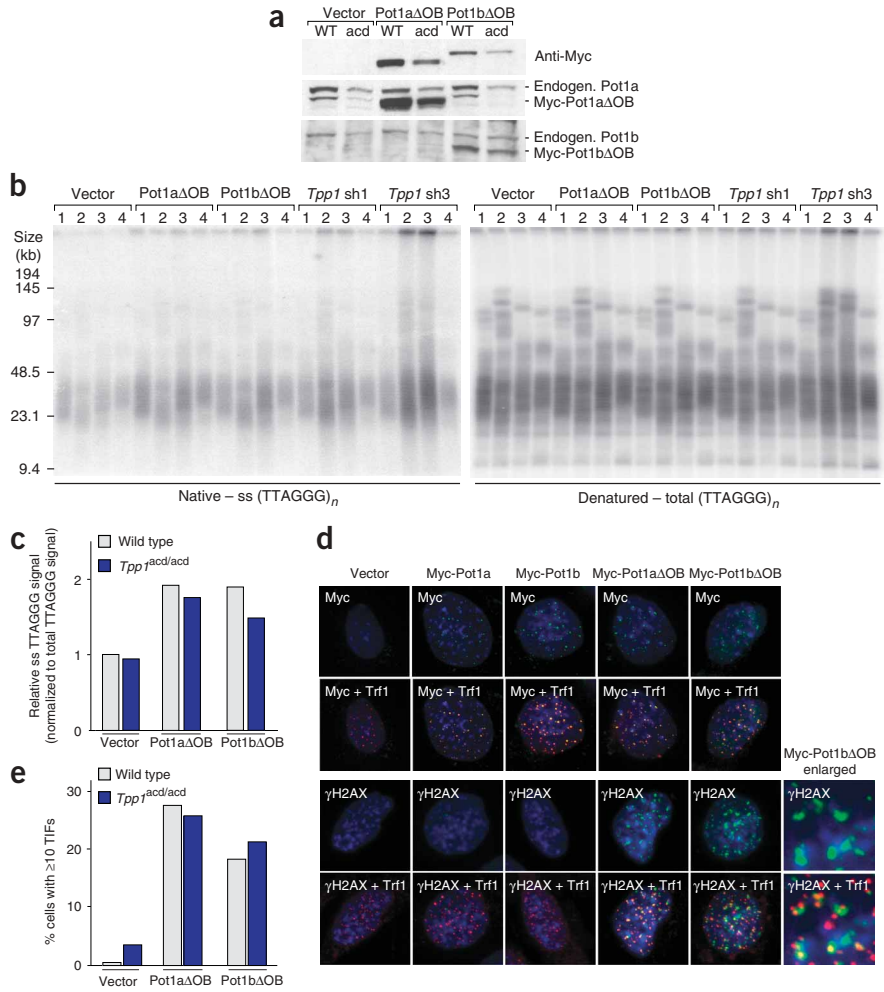

Figure 4 Dominant-negative interference between Pot1a and Pot1b. (**a**) Immunoblots analyzing expression of Myc-Pot1aΔOB and Myc-Pot1bΔOB in extracts of MEFs of the indicated *Tpp1* genotypes infected with pLPC-N-MycPot1aΔOB, pLPC-N-MycPot1bΔOB or control vector (pLPC N-Myc). Antibodies were as follows: top, Myc, 9E10; middle, Pot1a, 1221; bottom, Pot1b, 1223. Endogen., endogenous protein. (**b**) In-gel overhang assay (as in **Fig. 3c**) of wild-type (lanes 1 and 4) and $Tpp1^{acd/acd}$ (lanes 2 and 3) MEFs infected with control vector, vector expressing Pot1aΔOB or Pot1bΔOB (as in **a**), *Tpp1* shRNA 1 (sh1) or *Tpp1* shRNA 3 (sh3). Overhang assay was done after 5 d of selection with puromycin. (**c**) Quantification of the overhang signals from three independent wild-type or $Tpp1^{acd/acd}$ MEF cell lines expressing Pot1aΔOB, Pot1bΔOB or control vector as in **a**. (**d**) MEFs were infected with pLPC vectors expressing the indicated Myc-tagged proteins or with the empty pLPC-N-Myc vector, selected for 4 d with puromycin and immunofluorescently stained to detect Trf1 (red) and γ-H2AX (green). DNA was stained with DAPI (blue). (**e**) Quantification (as in **Fig. 3b**) of TIF-positive cells generated and analyzed as in **d**.

stability of TIN2 (ref. 19), which bridges TRF1 and TRF2 (refs. 11,14) and thereby contributes to the protection of telomeres from non-homologous end joining.

Dominant-negative interference between Pot1a and Pot1b

We speculated that if Pot1a and Pot1b both depend on Tpp1 for their ability to protect telomeres, overexpression of one of the Pot1 proteins might affect the function of the other. As it is not possible to substantially overexpress full-length Pot1, we tested this idea with *Pot1* alleles encoding proteins that lack the first OB fold but retain the Tpp1-binding domain (Pot1ΔOB), which can be overexpressed[16]. Analogous Pot1aΔOB and Pot1bΔOB proteins were generated, and these were found to accumulate at telomeres, as predicted from the retention of their Tpp1-binding domains (**Fig. 4** and data not shown). The expression of Pot1aΔOB was somewhat higher than that of Pot1bΔOB. Neither variant affected the nuclear localization of the endogenous Pot1 proteins (data not shown). Both Pot1aΔOB and Pot1bΔOB showed diminished expression in $Tpp1^{acd/acd}$ cells, consistent with their dependence on Tpp1 for stability (**Fig. 4a**). Pot1bΔOB induced a large increase in the amount of single-stranded telomeric DNA (**Fig. 4b**,**c**), as expected if Pot1b depends on Tpp1 for its ability to limit the length of the 3′ overhang. Pot1aΔOB induced TIFs, suggesting that Pot1aΔOB displaces Pot1a from Tpp1 (**Fig. 4d**,**e**). Notably, Pot1bΔOB expression also elicited a TIF response (**Fig. 4d**,**e**), which is a phenotype not observed in *Pot1b* knockout cells. Pot1aΔOB also induced aberrantly high overhang signals, a phenotype specific for Pot1b loss (**Fig. 4b**,**c**). The simplest interpretation of these data is that Pot1a and Pot1b both require Tpp1 for telomere protection and that the Tpp1-binding domains of Pot1aΔOB and Pot1bΔOB can displace the endogenous Pot1a and Pot1b from the telomeres.

This cross-competition can explain the recent results obtained with overexpression of a Pot1b variant deficient in DNA binding[8]. This protein induced end-to-end fusions and elicited a telomere DNA damage response, which are hallmarks of loss of Pot1a, not Pot1b. We propose that the Pot1b variant used in those studies diminishes the telomeric binding of Pot1a, acting similarly to the Pot1bΔOB proteins described here. Similarly, the cross-competition of a dominant-negative variant of Pot1a with Pot1b can explain the phenotype of the recently published *Pot1a* knockout[7]. The knockout strategy used in that study is predicted to generate a dominant-negative allele[6] and may therefore elicit a phenotype similar to that of the *Pot1a Pot1b* double knockout.

Human POT1 requires TPP1 to complement *Pot1a* knockout

We next used expression of human POT1 to test whether POT1 proteins can protect telomeres without the aid of TPP1. As shown above, human POT1 does not accumulate at mouse telomeres unless it is coexpressed with human TPP1 (or when mouse Tpp1 is highly overexpressed). To analyze the functional consequences of human POT1 expression (**Fig. 5**), we generated double-knockout MEFs lacking Pot1a and Pot1b that expressed human POT1 alone or in conjunction with TPP1. The presence of human POT1 and TPP1 largely rescued the proliferation defect of the double-knockout cells, whereas double-knockout cells containing either human POT1 or TPP1 alone proliferated as poorly as the vector control (**Fig. 5a**). The combined expression of human POT1 and TPP1 also repressed the endoreduplication phenotype associated with the loss of Pot1a and Pot1b, as shown by FACS analysis of the DNA content of the cells

(**Fig. 5b**) and determination of the total telomeric DNA signals in genomic blots loaded with equal numbers of cell equivalents (see below). The endoreduplication phenotype was completely absent from cells expressing both human POT1 and TPP1, whereas either protein alone had no effect (**Fig. 5b,e**). Finally, coexpression of human TPP1 and POT1 largely abrogated the formation of γ-H2AX and 53BP1 TIFs at mouse telomeres (**Fig. 5c,d**), indicating that the presence of human TPP1 and POT1 at telomeres allows mouse cells to make the distinction between DNA breaks and natural chromosome ends. Thus, human POT1 can protect mouse telomeres, but only in conjunction with TPP1.

Notably, in contrast to the complementation of the DNA damage response phenotypes of the *Pot1a Pot1b* double knockout, the combined expression of human TPP1 and POT1 did not result in appropriate control over the structure of the telomere terminus. *Pot1a Pot1b* double-knockout cells expressing both human TPP1 and POT1 continued to carry an excess of single-stranded telomeric DNA (**Fig. 5e,f**). Similar results were obtained with expression of human POT1 and TPP1 in *Pot1b* knockout cells (data not shown). The lack of overhang control by human POT1 and by mouse *Pot1a* suggests that the single-stranded DNA–binding activity of Pot1 is not sufficient to execute this function. Perhaps control of the overhang length requires a specific interaction between Pot1b and a mouse protein that cannot be bound by Pot1a or human POT1.

Trf2 affects telomeric association of Tpp1 and Pot1

The data presented above suggest that human and mouse Pot1 must interact with Tpp1 to carry out their protective functions. We next determined whether the Tpp1–Pot1 complexes are bound to telomeres in a manner that depends on other shelterin components, in particular Trf2. In human cells, inhibition of TRF2 with a dominant-negative allele indeed results in partial loss of POT1 at the telomere[16], but interpretation of this data is confounded by the fact that inhibition of TRF2 also removes part of the telomeric overhang[20]. Therefore, it is

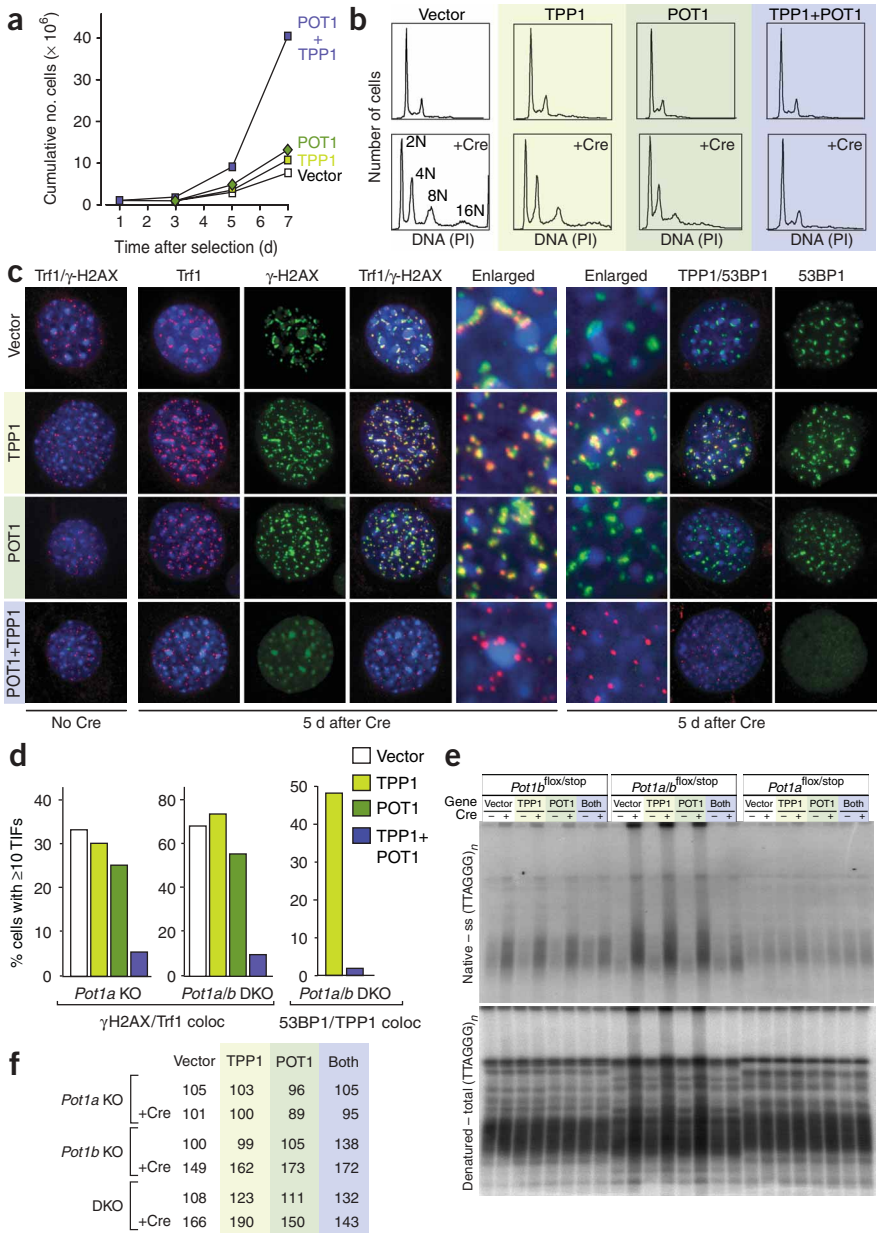

f

		Vector	TPP1	POT1	Both
Pot1a KO		105	103	96	105
	+Cre	101	100	89	95
Pot1b KO		100	99	105	138
	+Cre	149	162	173	172
DKO		108	123	111	132
	+Cre	166	190	150	143

Figure 5 Human POT1 complements Pot1a loss when coexpressed with human TPP1. (**a**) Growth curve of *Pot1a Pot1b* double-knockout MEFs complemented with POT1 and TPP1 after the deletion of Pot1a and Pot1b with adenoviral Cre. Before Cre infection, *Pot1a*$^{stop/flox}$ *Pot1b*$^{stop/flox}$ cells were infected with pWzl-N-MycPOT1 or the empty pWzl-N-Myc vector and selected with hygromycin. Subsequently, cells were infected with pLPC-N-FlagTPP1 or the empty pLPC-N-Flag vector. No selection was applied because of puromycin resistance of the double-knockout cells. TPP1 infection efficiency was >80% in all infections. Cellular arrest and senescent morphology of the *Pot1a Pot1b* double knockout (data not shown) is rescued in cells infected with both POT1 and TPP1. (**b**) FACS profiles of *Pot1a Pot1b* double-knockout MEFs infected as in **a**. Cells were infected with a Hit&Run Cre retrovirus[6] to delete Pot1a and Pot1b as indicated. Cells were gated to remove sub-G1 peaks. N, ploidy; PI, propidium iodide stain. (**c**) TIF assay of cells in **a**. Immunofluorescent staining of Trf1 (red) and γ-H2AX (green) or the Flag tag of human TPP1 (red) and 53BP1 (green) was used to detect cells that were successfully transduced with TPP1 and contained 53BP1 foci at their telomeres. DNA was stained with DAPI (blue) (**d**) Quantification (as in **Fig. 3b**) of TIF-positive cells in **c**. Left, *Pot1a* knockout strain; middle, *Pot1a Pot1b* double-knockout strain; right, 53BP1 colocalizing (coloc) with transduced Flag-tagged human TPP1 in double-knockout cells with and without human POT1. (**e**) In-gel overhang assays (as in **Fig. 3c**) of *Pot1b* knockout (KO), *Pot1a Pot1b* double-knockout (*Pot1a/b* DKO) and *Pot1a* KO cells retrovirally transduced with pWzl-N-MycPOT1, pLPC-N-FlagTPP1 or vector as in **a**. *Pot1* genes were deleted using Hit&Run Cre retrovirus and overhang lengths were determined 5 d after infection. Lanes were loaded with the same cell number equivalents. Lanes containing DNA from *Pot1a/b* DKO cells after Cre treatment show increased telomeric signals owing to endoreduplication. (**f**) Quantification of telomeric overhang signal in **e**. The relative overhang signal of *Pot1b* KO cells before Cre treatment was set at 100.

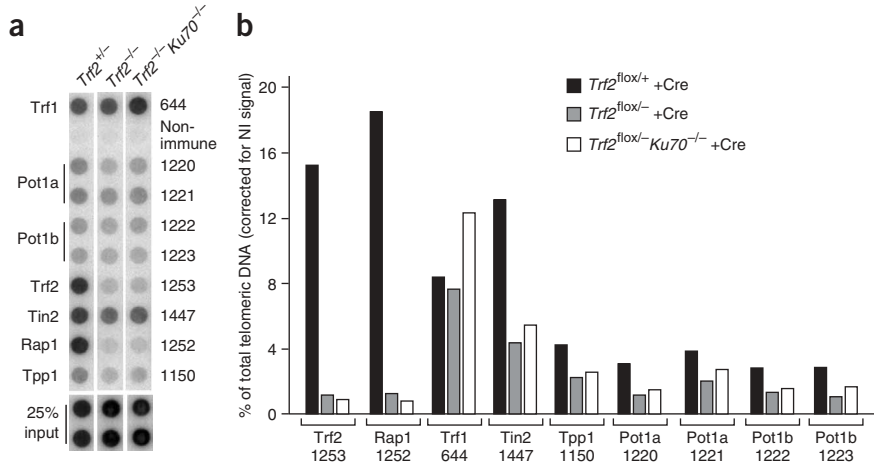

Figure 6 Trf2 affects the telomeric accumulation of Pot1a and Pot1b. (**a**) Telomeric ChIP analysis of cells lacking Trf2. Listed genotypes refer to the genotype at the time of the ChIP experiment, which was done after infection with pWzl-Cre and selection in hygromycin for 5 d. The pre-recombination (floxed) genotypes were, from left to right, *Trf2*$^{flox/+}$, *Trf2*$^{flox/-}$, and *Trf2*$^{flox/-}$ *Ku70*$^{-/-}$. Proteins and antibodies used in the ChIPs are indicated next to the dot-blots. (**b**) Quantification of percentages of total telomeric DNA recovered in ChIPs shown in **a**. NI, nonimmune.

not possible to distinguish between effects on the protein interactions of POT1 and effects on its binding to the single-stranded telomeric DNA. To further examine the contribution of Trf2 to the recruitment of Tin2, Tpp1 and Pot1 to telomeres, we used *Terf2*$^{flox/-}$ MEFs (*Terf2*, encoding Trf2 protein, is also called *Trf2*) from which Trf2 can be deleted with Cre[21]. When Trf2 is deleted in *Xrcc6* $^{-/-}$ cells (*Xrcc6* is also called *Ku70*), the telomere fusion phenotype typical of Trf2 deficiency is largely abrogated, and, importantly, the telomeric overhang remains intact[22]. Therefore, in this setting, the effect of Trf2 on the telomeric recruitment of Pot1 can be determined without the confounding aspects of overhang loss. ChIP analysis of *Trf2*$^{flox/-}$ *Ku70*$^{-/-}$ cells showed the expected loss of Trf2 and its interacting factor Rap1 from telomeres (**Fig. 6**). Trf1 was not affected, but the telomeric association of Tin2, Tpp1, Pot1a and Pot1b were somewhat reduced (**Fig. 6**). These data indicate that telomeric accumulation of Tin2–Tpp1–Pot1 is in part dependent on Trf2. Previous data from human cells have supported for a role of TRF1 in the telomeric association of POT1 (ref. 16). Mouse cells lacking both Trf1 and Trf2 will be required to establish whether recruitment of Pot1a and Pot1b is entirely dependent on the duplex telomeric DNA–binding proteins.

DISCUSSION

Several lines of evidence indicate that Pot1 requires an interaction with Tpp1 to fulfill its protective function. Mouse Pot1a and Pot1b are dependent on Tpp1 for their detectable recruitment to telomeres, and removal of Tpp1 from mouse telomeres results in telomere-deprotection phenotypes indicative of impaired function of Pot1a and Pot1b. Human POT1 by itself does not bind or protect mouse telomeres, but when coexpressed with human TPP1 or an excess of mouse Tpp1, human POT1 can fulfill the functions of Pot1a. Finally, neither mouse nor human Tpp1 is capable of protecting telomeres when Pot1 is not present. Collectively, the findings indicate that neither Pot1 nor Tpp1 is sufficient to protect telomeres without its partner: full protection requires the interaction of both proteins at telomeres. Our data are consistent with a recent report indicating that compromised TPP1 function can elicit a DNA damage response at telomeres[23], although this study did not distinguish between effects on telomere protection by TRF2 and by POT1. It remains to be determined whether the dependence of Pot1 on Tpp1 simply reflects Tpp1's ability to position Pot1 at telomeres or involves additional attributes of Tpp1.

We envisage two alternative models for the protective functions of Pot1 and Tpp1. In one model, Pot1 and Tpp1 act together but independent of the rest of the shelterin complex. Pot1 and Tpp1 might be able to associate with the single-stranded telomeric DNA, either at the 3′ overhang or in the D loop, when telomeres are in the t-loop configuration[24]. The presence of the Pot1–Tpp1 heterodimer on the single-stranded DNA might be sufficient to repress a DNA damage signal, inappropriate repair reactions and formation of excessive single-stranded DNA. None of our data excludes this model. A second model, which we prefer, is that Tpp1 serves (in part) to connect Pot1 to the duplex part of the telomere. According to this model, Pot1 would protect telomeres as part of the shelterin complex. As shelterin is extremely abundant at chromosome ends, a large number of Tpp1 and Pot1 molecules could be positioned near the single-stranded telomeric DNA. Regardless of the exact configuration of the double-stranded and single-stranded telomeric DNA, the high density of shelterin at chromosome ends is likely to improve the association of the Pot1 OB folds with single-stranded telomeric DNA. This effect may be biologically relevant, as the single-stranded telomeric DNA is also expected to be a substrate for binding by RPA, an abundant nuclear protein complex involved in DNA damage signaling. Pot1 and RPA are therefore expected to compete for the single-stranded DNA at the telomere terminus or in the D loop, and the association of Pot1 with the rest of the shelterin complex may provide a competitive advantage to Pot1. Competition for RPA on single-stranded telomeric DNA may be particularly important for mammalian cells, which have long ($\geq$50 nt) single-stranded telomeric overhangs. Many eukaryotes have telomeric overhangs that are shorter than the minimal RPA-binding site (30 nt) for most of the cell cycle. Examples are *Saccharomyces cerevisiae*, *Schizosaccharomyces pombe* and ciliates. It is noteworthy that in these organisms, binding of the single-stranded telomeric DNA-binding complex seems to be independent of the proteins associated with the duplex telomeric DNA. Thus, the connection of Pot1 and Tpp1 to Trf1 and Trf2 may be a special adaptation to the long 3′ terminus at mammalian telomeres.

The functional relationship of Pot1 and Tpp1 is consistent with the recent proposal that these factors are related to ciliate TEBPα and TEBPβ[9,23]. Despite their ancient origin, the mammalian Pot1 proteins diverge rapidly. The preeminent example of this divergence is the acquisition of a second Pot1 gene in rodents. The copy number difference between rodents and other mammals is unlikely to be due to a gene deletion, which would have had to occur more than once to explain the single Pot1 gene of chicken, *Xenopus laevis* and most mammals. We also consider it unlikely that the sequenced nonrodent genomes contain an unrecognized second Pot1 gene, because the missing Pot1 is expected to have at least 70% sequence identity to its homologs. Thus, the most parsimonious interpretation is that the two Pot1 proteins of rodents originate from a recent (~75 million years) gene duplication[6]. In addition to the Pot1 gene

duplication, the divergence of human and mouse Pot1 apparently affects their interaction with Tpp1, such that human POT1 interacts better with human TPP1 than with the mouse version. Our data also hint at a functional divergence of human and mouse Pot1. Whereas human TPP1 and POT1 appear to effectively complement the loss of Pot1a, the human proteins do not take on the role of Pot1b in limiting the amount of single-stranded telomeric DNA. The question of whether Pot1b has evolved a new function not represented by human POT1 will require further analysis. Together, the data illuminate recent (75 million years) variations on telomere machinery that has functioned at chromosome ends for at least 1.5 billion years.

METHODS

Cell lines. Cre-mediated conditional deletion of Pot1a, Pot1b and Trf2 in wild-type or Ku70-deficient MEFs was described[6,22]. *Tpp1*$^{acd/acd}$ MEFs were isolated on embryonic day 13.5 from crosses of *Tpp1*$^{acd/+}$ mice on a mixed background produced by a cross of DW/J with BL6. Embryos were genotyped as described[18].

Immunoblotting, immunofluorescence and chromatin immunoprecipitation. Procedures for immunoblotting, immunofluorescence and ChIP were described[6]. Pot1a was detected using affinity-purified antibody 1221, and Pot1b was detected using purified 1223. The Flag epitope tag of TPP1 was detected with mouse anti-Flag M2 (Sigma), and the Myc epitope of POT1 constructs was detected with mouse anti-Myc 9E10 (Sigma) in immunoblots and immunofluorescence. TPP1 antibodies were produced in rabbits immunized with a glutathione *S*-transferase (GST) fusions of a human TPP1 fragment spanning amino acid residues 1–250 (antibody 1150) or 250–544 (antibody 1151). For cell-fractionation experiments, cells were lysed in 10 mM HEPES (pH 7.4), 0.1% (v/v) Triton X-100, 10 mM KCl, 1.5 mM MgCl, 340 mM sucrose, 10% (v/v) glycerol, 1 mM DTT and 1 mM PMSF. After 10 min on ice, the supernatants, containing cytoplasmic proteins, were collected by centrifugation at 4,000 r.p.m. in an Eppendorf microfuge for 4 min. To obtain the nucleoplasmic fractions, pellets were resuspended in 50 mM Tris-HCl (pH 7.4), 1% (v/v) Triton X-100, 0.1% (w/v) SDS, 400 mM NaCl and 1 mM EDTA, and incubated on ice for 10 min. Insoluble components were separated by centrifugation at 13,000 r.p.m. for 10 min.

Telomeric overhang assay. Telomere overhangs were analyzed as described[6]. Signals were quantified and the single-stranded telomeric signal (from probing of native DNA) was normalized to total telomeric DNA signal (from probing of denatured DNA) in the same lane. The normalized values were compared between samples.

Retroviral transduction. Retroviral transduction was done as described[6]. The human *POT1* complementary DNA[16] was subcloned using BamHI and XhoI restriction sites ligated to BamHI- and SalI-digested pWzl-Myc retroviral vector. The human pLPC-FlagTPP1 was described[12]. shRNAs targeting *Tpp1* were expressed using the pSuperior retroviral expression vector (OligoEngine). Target sequences were as follows: Tpp1-1, 5′-GTAGCTTGGGCCTTGAATA-3′; Tpp1-2, 5′-GAACCGGGCAGCTGCTCAA-3′; Tpp1-3, 5′-GGACACATGGGCTGACGGA-3′. Genes encoding Pot1aΔOB and Pot1bΔOB were cloned into pLPC-N-Myc using the following PCR primers: Pot1aΔOB fw, 5′-ACCTGGATCCCCTCAGGACCAAAAAATGGTAG-3′; Pot1aΔOB rev, 5′-ACCTCTCGAGCTAGACAACATTTTCTGCAACTG-3′; Pot1bΔOB fw, 5′-ACCTGGATCCGCTCAGGACTACAGTATGGTAG-3′; Pot1bΔOB rev, 5′-ATGCGTCGACATCATAGTTACTTTCTGGTAAG-3′.

Note: Supplementary information is available on the Nature Structural & Molecular Biology website.

ACKNOWLEDGMENTS

We thank M. Lei for communicating his findings on the structure of TPP1 before publication, and E. Lazzerini Denchi, K. Hoke and A. Sfeir for insightful comments on this manuscript. J.-P.D. and W.P. were supported by the Studienstiftung des deutschen Volkes. D.H. was supported by a Cancer Research Institute Predoctoral Emphasis Pathway in Tumor Immunology Grant and Rockefeller University Graduate Program Funds. T.E. was supported by the Deutche Forschungsgemeinschaft (DFG EL265/I). This work was supported by grants from the US National Institutes of Health to T.d.L. (GM49046 and CA76027), G.D.H. (DK62027 and DK65313) and C.E.K. (K08-HD42487) and by a March of Dimes Basil O'Connor Award to C.E.K.

AUTHOR CONTRIBUTIONS

D.H. designed and performed the experiments, with W.P. contributing in the later stages of the project. J.-P.D. and K.K.T. contributed to the experiments in the supplementary figures. G.D.H., C.E.K. and T.E. generated the *Tpp1*$^{acd/acd}$ cells used in this study. J.Z.-S.Y. generated the TPP1 antibodies. T.d.L. wrote the paper and made the figures.

COMPETING INTERESTS STATEMENT

The authors declare no competing financial interests.

Published online at http://www.nature.com/nsmb/
Reprints and permissions information is available online at http://npg.nature.com/reprintsandpermissions

1. de Lange, T. Shelterin: the protein complex that shapes and safeguards human telomeres. *Genes Dev.* **19**, 2100–2110 (2005).
2. Baumann, P. & Cech, T.R. Pot1, the putative telomere end-binding protein in fission yeast and humans. *Science* **292**, 1171–1175 (2001).
3. Veldman, T., Etheridge, K.T. & Counter, C.M. Loss of hPot1 function leads to telomere instability and a cut-like phenotype. *Curr. Biol.* **14**, 2264–2270 (2004).
4. Yang, Q., Zheng, Y.L. & Harris, C.C. POT1 and TRF2 cooperate to maintain telomeric integrity. *Mol. Cell. Biol.* **25**, 1070–1080 (2005).
5. Hockemeyer, D., Sfeir, A.J., Shay, J.W., Wright, W.E. & de Lange, T. POT1 protects telomeres from a transient DNA damage response and determines how human chromosomes end. *EMBO J.* **24**, 2667–2678 (2005).
6. Hockemeyer, D., Daniels, J.P., Takai, H. & de Lange, T. Recent expansion of the telomeric complex in rodents: two distinct POT1 proteins protect mouse telomeres. *Cell* **126**, 63–77 (2006).
7. Wu, L. *et al.* Pot1 deficiency initiates DNA damage checkpoint activation and aberrant homologous recombination at telomeres. *Cell* **126**, 49–62 (2006).
8. He, H. *et al.* POT1b protects telomeres from end-to-end chromosomal fusions and aberrant homologous recombination. *EMBO J.* **25**, 5180–5190 (2006).
9. Wang, F. *et al.* The POT1–TPP1 telomere complex is a telomerase processivity factor. *Nature* **445**, 506–510 (2007).
10. Kim, S.H., Kaminker, P. & Campisi, J. TIN2, a new regulator of telomere length in human cells. *Nat. Genet.* **23**, 405–412 (1999).
11. Ye, J.Z. *et al.* TIN2 binds TRF1 and TRF2 simultaneously and stabilizes the TRF2 complex on telomeres. *J. Biol. Chem.* **279**, 47264–47271 (2004).
12. Ye, J.Z. *et al.* POT1-interacting protein PIP1: a telomere length regulator that recruits POT1 to the TIN2/TRF1 complex. *Genes Dev.* **18**, 1649–1654 (2004).
13. Liu, D. *et al.* PTOP interacts with POT1 and regulates its localization to telomeres. *Nat. Cell Biol.* **6**, 673–680 (2004).
14. Kim, S.H. *et al.* TIN2 mediates functions of TRF2 at human telomeres. *J. Biol. Chem.* **279**, 43799–43804 (2004).
15. Houghtaling, B.R., Cuttonaro, L., Chang, W. & Smith, S. A dynamic molecular link between the telomere length regulator TRF1 and the chromosome end protector TRF2. *Curr. Biol.* **14**, 1621–1631 (2004).
16. Loayza, D. & de Lange, T. POT1 as a terminal transducer of TRF1 telomere length control. *Nature* **423**, 1013–1018 (2003).
17. Smogorzewska, A. & de Lange, T. Regulation of telomerase by telomeric proteins. *Annu. Rev. Biochem.* **73**, 177–208 (2004).
18. Keegan, C.E. *et al.* Urogenital and caudal dysgenesis in adrenocortical dysplasia (acd) mice is caused by a splicing mutation in a novel telomeric regulator. *Hum. Mol. Genet.* **14**, 113–123 (2005).
19. O'Connor, M.S., Safari, A., Xin, H., Liu, D. & Songyang, Z. A critical role for TPP1 and TIN2 interaction in high-order telomeric complex assembly. *Proc. Natl. Acad. Sci. USA* **103**, 11874–11879 (2006).
20. van Steensel, B., Smogorzewska, A. & de Lange, T. TRF2 protects human telomeres from end-to-end fusions. *Cell* **92**, 401–413 (1998).
21. Celli, G.B. & de Lange, T. DNA processing not required for ATM-mediated telomere damage response after TRF2 deletion. *Nat. Cell Biol.* **7**, 712–718 (2005).
22. Celli, G.B., Lazzerini Denchi, E. & de Lange, T. Ku70 stimulates fusion of dysfunctional telomeres yet protects chromosome ends from homologous recombination. *Nat. Cell Biol.* **8**, 885–890 (2006).
23. Xin, H. *et al.* TPP1 is a homologue of ciliate TEBP-beta and interacts with POT1 to recruit telomerase. *Nature* **445**, 559–562 (2007).
24. Griffith, J.D. *et al.* Mammalian telomeres end in a large duplex loop. *Cell* **97**, 503–514 (1999).

selection with puromycin, cells were analyzed by IF for Trf1 (Ab 644, red) and the Myc epitope tag of Pot1b (9E10, green) and counter stained with DAPI (blue).

(c) Subcellular localization of the Pot1b versions described in (a) in Pot1b KO cells. The nuclear control represents an unknown nuclear protein of ~100 KDa detected with the Rap1 antibody 1252. Similar results were obtained in wild type cells (data not shown).

Supplemental Figure 2. Hockemeyer et al.

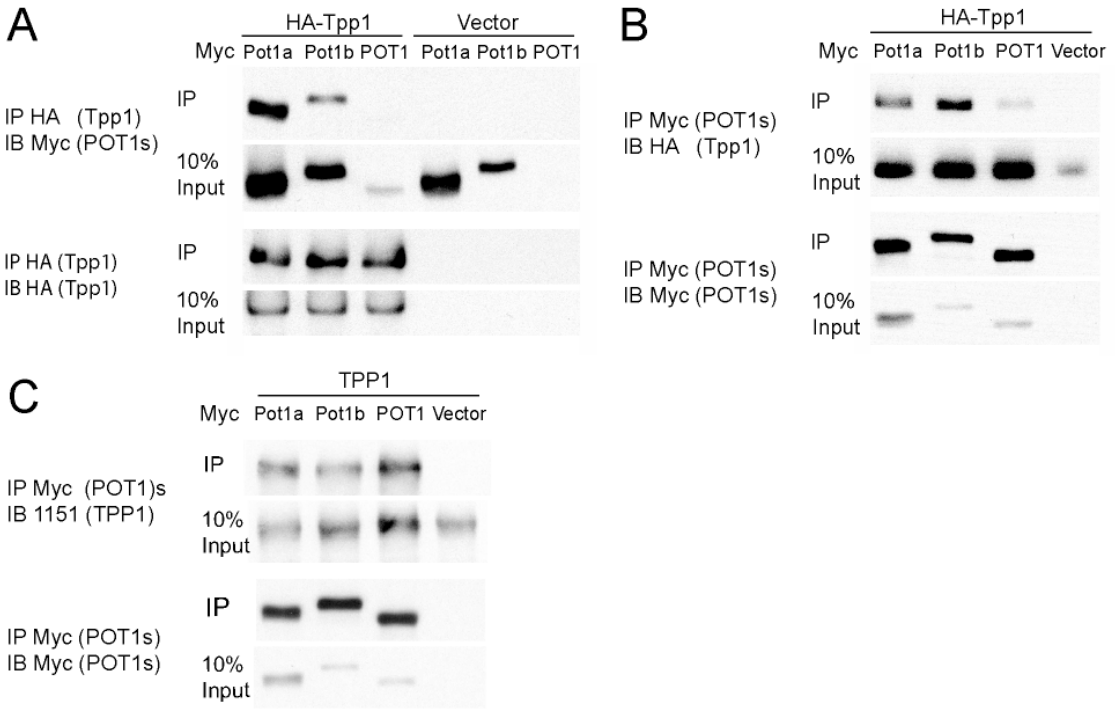

Supplemental Figure 2. Interaction of human and mouse POT1 and TPP1 proteins

(a) Coimmunoprecipitation of mouse Pot1a/b and human POT1 with mouse Tpp1. HA-Tpp1, MycPot1a, MycPot1b, or MycPOT1 (human) were was transiently cotransfected into 293T cells as indicated. Whole cell extracts (input) were immunoprecipitated (IP) using an anti-HA antibody. Abs: Myc, 9E10; HA, 3F10.

(b) Coimmunoprecipitation of mouse Tpp1 with mouse Pot1a/b and human POT1. As in (a) but whole cell extracts (input) were immunoprecipitated (IP) using an anti-Myc antibody.

(c) Coimmunoprecipitation of human TPP1 with mouse Pot1a/b and human POT1. MycPot1a, MycPot1b or MycPOT1 was transiently cotransfected into 293T cells together

with human TPP1. Whole cell extracts (input) were immunoprecipitated (IP) using an anti-Myc antibody. Shown are immunoblots for input and precipitated Myc tagged proteins (Myc, 9E10) and human TPP1 (1151).

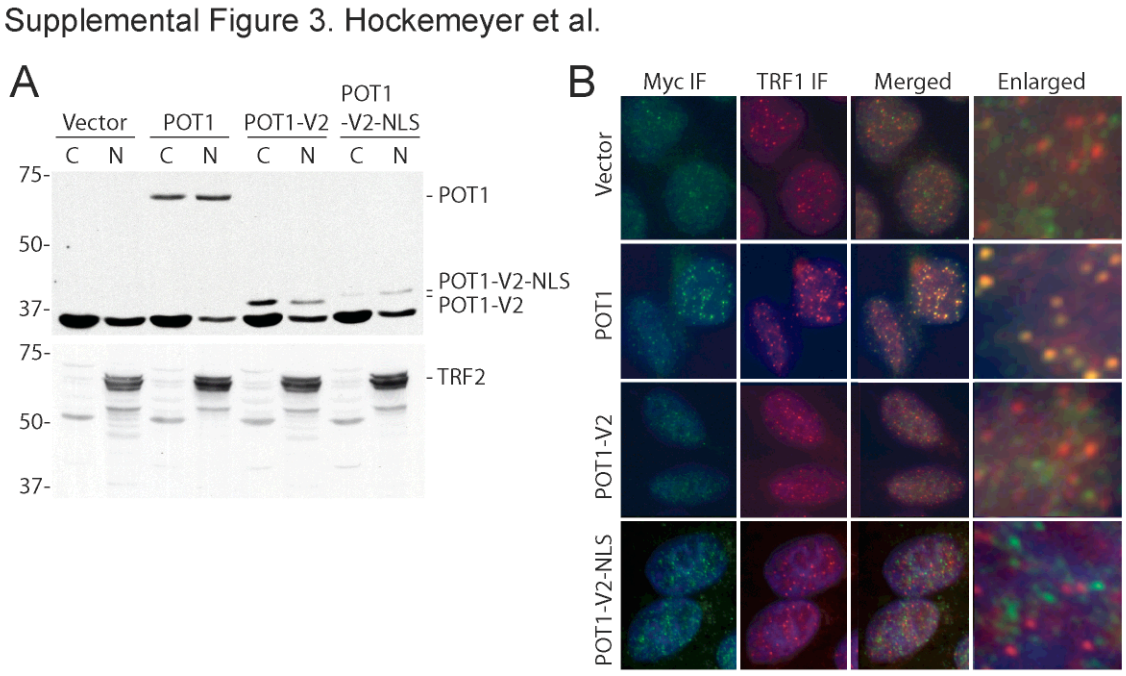

Supplemental Figure 3. Subcellular localization of human POT1 variants lacking the TPP1 interaction domain.

(a) IF of ectopically expressed human POT1. Myc-tagged variants of human POT (full length, V2, V2-NLS) were expressed in Hela1.2.11 cells using retroviral transduction. After selection with puromycin cells were analyzed by IF for TRF1 (371, red) and the Myc epitope tag of POT1 (9E10, green). DNA was stained with DAPI (blue).

(b) Subcellular localization of the POT1 versions described in (a). The nuclear control is human TRF2. Abs: Myc, 9E10; TRF2, 647.

Supplemental Figure 4. Hockemeyer et al.

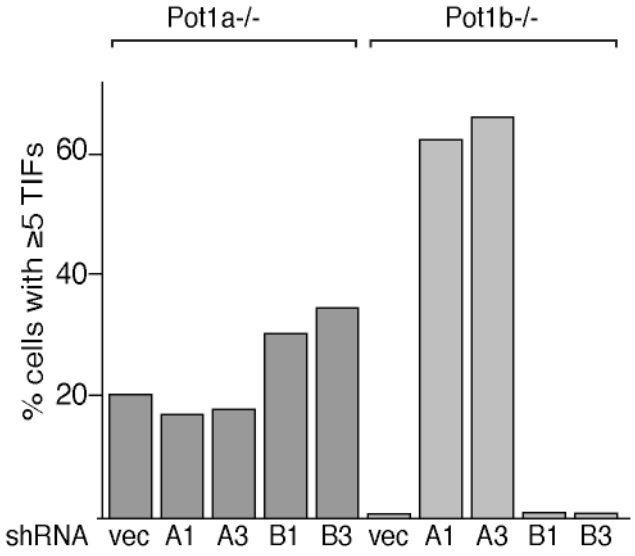

Supplemental Figure 4. Validation of the Pot1a and Pot1b knockout strategies using shRNA mediated depletion of Pot1a and Pot1b.

Pot1a-/- cells and Pot1b-/- cells (post-Cre) were infected with a vector control (vec) or two independent shRNA retroviral constructs targeting either Pot1a (A1 and A3) or Pot1b (B1 and B3). Cells were analyzed for TIFs by IF for Trf1 and 53BP1. Cells with more that 5 TIFs were counted as TIF positive. While the knockdown of Pot1b in Pot1a-/- cells results in an increase in TIF positive cells, depletion of Pot1a does not. In Pot1b-/- cells the knockdown of Pot1b does not result in TIF formation, but knockdown of Pot1a results in a TIF phenotype similar to that of Pot1a/b DKO cells.